Vibrational State-Resolved Study of the $O^- + D_2$ Reaction: Direct Dynamics from 0.47 to 1.20 eV†

M. A. Carpenter‡ and J. M. Farrar*

Department of Chemistry, University of Rochester, Rochester, New York 14627

Received: June 4, 1997⊗

We present a crossed beam study of the title reaction over the collision energy range from 0.47 to 1.20 eV, over which the dynamics of particle transfer are direct. The data include vibrational state populations and vibrational-state dependent angular distributions. Over the entire collision energy range, the product vibrational state distributions are inverted, and the extent of that inversion as measured by the vibrational surprisal increases with increasing collision energy. The energy dependence of the product vibrational state distributions is partially consistent with mixed energy release in the Heavy + Light−Light mass combination, but it more closely resembles the behavior of proton transfer in the $O^- + HF$ system at low energies, where the attractive well induces corner cutting trajectories, leading to partitioning of increased reagent translation into product vibration. The most probable rotational energy is approximately constant as a function of vibrational quantum number and is effectively independent of collision energy. This saturation effect is consistent with the softening of the low energy repulsive wall as the collision geometry changes from collinear to bent. Several features of the data can be rationalized with extant *ab initio* calculations, but other features, especially the vibrational state populations, require additional theoretical insight for complete understanding.

I. Introduction

The study of elementary ion-neutral reaction dynamics is a field that has experienced intense activity over the last two decades. In providing an intellectual foundation for the application of simple dynamical concepts to practical, complex systems where such reactions are important, *e.g.*, atmospheric chemistry, combustion, and electrical discharges, one seeks prototypical systems for detailed study. Such systems should be those for which detailed, state-resolved cross sections can be measured, *ab initio* potential energy surfaces of reasonable accuracy can be computed, and reliable dynamical calculations on those surfaces can be performed. The simplicity of chemical reactions involving atom transfer from the hydrogen molecule and its isotopomers has made such systems among the most widely studied prototypes, both theoretically and experimentally. In two recent publications[1,2] we reported an example of such a system, including detailed differential cross sections, resolved in the vibrational states of the products, for the deuterium atom transfer reaction between O^- and molecular deuterium over a range of collision energies up to 1.20 eV:

$$O^- + D_2 \rightarrow OD^- + D + 0.30\ \text{eV} \qquad (1)$$

Over the collision energy range from 0.25 to 0.37 eV, the ground and first excited vibrational states of the OD^- products are accessible by energy conservation, and a number of dynamical features unify the cross sections. In particular, we found that the angular distributions for the individual product vibrational states differ consistently: the $v' = 0$ state shows a distribution with both forward and backward scattered components, while products formed in $v' = 1$ are scattered primarily in the forward direction. At the lowest collision energy of 0.25 eV, we found that the products show a sharp spike in the backward direction, suggesting that collinear collisions become especially important in that energy regime. We also found that the vibrational surprisal,[3] a measure of the deviation of the measured state probabilities in comparison with a microcanonical "prior" distribution, was always negative, increasing in magnitude with increasing collision energy, but extrapolating to a positive value at very low collision energy.

The interpretation of these data was greatly facilitated by an *ab initio* calculation performed by Werner, Mänz, and Rosmus[4] that focused on the stability of the $[H_2O]^-$ anion, but also addressed the nature of the $O^- + H_2$ and $OH^- + H$ channels that lead to this species. The calculations show that approaching $O^- + H_2$ reactants correlate to $OH^-(^2\Sigma^+) + H(^2S_{1/2})$ along a collinear $^2\Sigma^+$ surface. This $^2\Sigma^+$ surface has two shallow local minima separated by a barrier. The first shallow well arises from the electrostatic attraction of O^- with the quadrupole moment of H_2 in a collinear $O^-\cdots HH$ geometry. Hydrogen atom transfer to a second local minimum, having the structure $OH^-\cdots H$, occurs over a small barrier. Decomposition of this second complex, formally a saddle point on the potential energy surface, leads to the products $OH^- + H$. The calculations show that bending motion at this saddle point defines the coordinate leading to associative detachment[5,6] forming $H_2O + e^-$, a channel exothermic by 3.6 eV. Noncollinear geometries near the $OH^-\cdot H$ saddle point access the $H_2O + e^-$ continuum without a barrier.

As applied to our experiments in the collision energy range from 0.25 to 0.37 eV, the *ab initio* calculations show that motion through the region of the $OH^-\cdot H$ saddle point is critical in determining the branching between particle transfer and associative detachment, further playing a role in the vibrational state distributions of the products and in the low energy angular distributions. At low collision energies, the transit time of the nuclei through the $OH^-\cdot H$ saddle in comparison with the autoionization lifetime, given by $\hbar/\Gamma(R)$, determines the fraction of the collisions that are channeled into electron detachment. In the low-energy limit, only collinear collisions lead to particle transfer, as noncollinear collisions lead to bending motion on a

† Originally submitted as part of the Y. T. Lee Festschrift issue [*J. Phys. Chem. A* **1997**, *101* (36)].

‡ Present address: Baker Chemical Laboratory, Cornell University, Ithaca, NY 14853.

⊗ Abstract published in *Advance ACS Abstracts,* August 1, 1997.

S1089-5639(97)01828-8 CCC: $14.00

timescale comparable to the time of passage through the OH^-·H saddle and electron detachment occurs. This restriction in collision geometries also leads to "cooler" product vibrational state distributions than expected statistically. Over the collision energy range from 0.25 to 0.37 eV, the fraction of the available energy in product vibration remains constant at 30%, but the distribution shows a monotonically increasing bias toward $v' = 1$ with increasing collision energy.

In the higher energy regime, a few previous studies employing ion beam techniques have yielded measurements of product energy disposal and angular distributions that have probed the potential surface in the attractive and low energy repulsive regions. Herbst *et al.*[7] employed an ion beam/scattering cell arrangement to examine atom transfer and electron detachment over the collision energy range from 3.6 to 13.2 eV. The OD^- product was found to be predominately forward-scattered throughout this energy range, a result consistent with our preliminary report.[2] "Trajectory surface leaking" calculations down to collision energies of 1.2 eV reproduced this observation. Cross and collaborators[8] examined the atom transfer channel 1 over a lower collision energy range from 1.2 to 4.7 eV and observed impulsive dynamics forming forward scattered OD^- products at the higher end of the energy range. The experimental data also suggested that the reaction proceeded through the intermediacy of a transient complex living approximately a rotational period at the lower end of this energy range, although the work of Herbst as well as that of our own group[2] shows that this conclusion is in error.

As part of our continuing study of reaction 1, we report in this paper a study of the differential cross sections over the collision energy range from 0.47 to 1.20 eV. Many of the trends that began to evidence themselves at lower collision energy continue to develop, providing further probes of the potential surface for reaction, principally in the low-energy repulsion. In this paper we present a full account of energy disposal and product angular distributions for the reactively scattered OD^- products of reaction 1 over this range. The data include vibrational state distributions at each collision energy, angular distributions for individual quantum states of the products, and estimates of the most probable rotational energy of the products within individual vibrational states. The experimental data overlap the work of Cross and collaborators at the upper end of the collision energy range and extend the study to much lower collision energies where dynamical features that probe details of the potential energy surface come into play.

II. Experimental Section

The crossed beam apparatus used for this study has been described in detail in previous publications.[9] We produced O^- ions by electron impact on N_2O at a pressure of ~0.01 Torr, and we formed the beam of reagent ions with a magnetic mass spectrometer. The ion beam laboratory energy distribution was approximately triangular in shape, with a full width at half-maximum of ~0.25 eV. Center of mass collision energies ranging from 0.47 to 1.20 eV required lab energy beams ranging from 2.04 to 5.60 eV. The neutral beam was produced by expanding 560 Torr of D_2 at 300 K through a 0.07 mm nozzle, by collimating the beam to 2° by a 1 mm electroformed skimmer and a 3.5 mm square aperture, and by modulating it at 30 Hz. Under these conditions, we estimate that the D_2 rotational temperature is 195 K[10] and the rotational energy of the D_2 reagents is only 0.01 eV.

The beams intersected at the center of a collision chamber maintained at 10^{-7} Torr with oil diffusion pumps. Reaction products were detected with a rotatable electrostatic energy analyzer−quadrupole mass filter equipped with a dual microchannel plate ion detector. Data were collected with a computer-controlled multichannel scaler synchronized with the beam modulation.[11] The energy scale was calibrated at the beginning and at the end of each experiment by resonant charge transfer from NO^-, also produced by electron impact on N_2O, to NO expanded supersonically in the crossed beam. This calibration procedure generated a low energy marker at the energy of the neutral beam, ~0.09 eV. All experimental data were duplicated, and experiments in which the energy of the primary ion beam drifted by more than 0.1 eV were discarded.

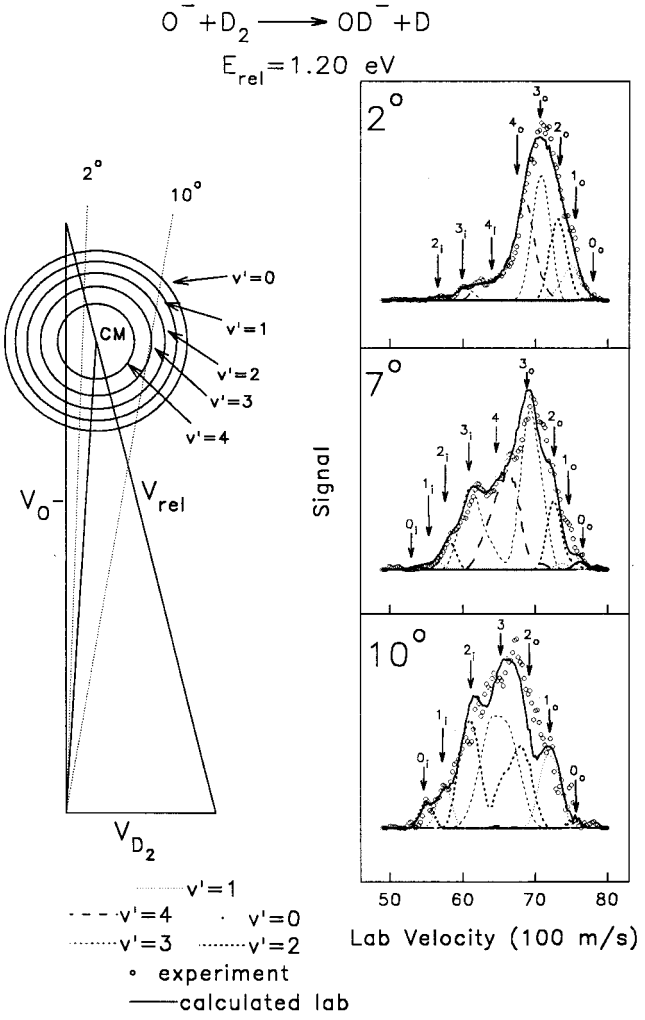

Figure 1. Experimental data for OD^- lab flux distributions at selected laboratory angles at a collision energy of 1.20 eV. At each lab angle, structure in the fluxes is assigned to specific vibrations. The integer above the arrow pointing to a given structure identifies the vibrational quantum number of the OD^- product appearing at that angle and velocity. The subscripts "i" and "o" denote the inner and outer branches of the kinematic circles shown on the Newton diagram. The results of the kinematic simulation of the data are shown at each angle, with contributions from individual vibrational states indicated.

III. Results and Analysis

The particle transfer reaction 1 was studied at collision energies of 0.47, 0.85, and 1.20 eV. At each collision energy, laboratory kinetic energy spectra were obtained at a set of 12−15 fixed lab scattering angles. Each energy spectrum consisted of 80 or 120 points, with typical energy bin widths of 0.025−0.03 eV, compared to the laboratory resolution of 0.07 eV. This procedure resulted in a data set consisting of 960−1800 data points covering laboratory velocity space. Figure 1 shows

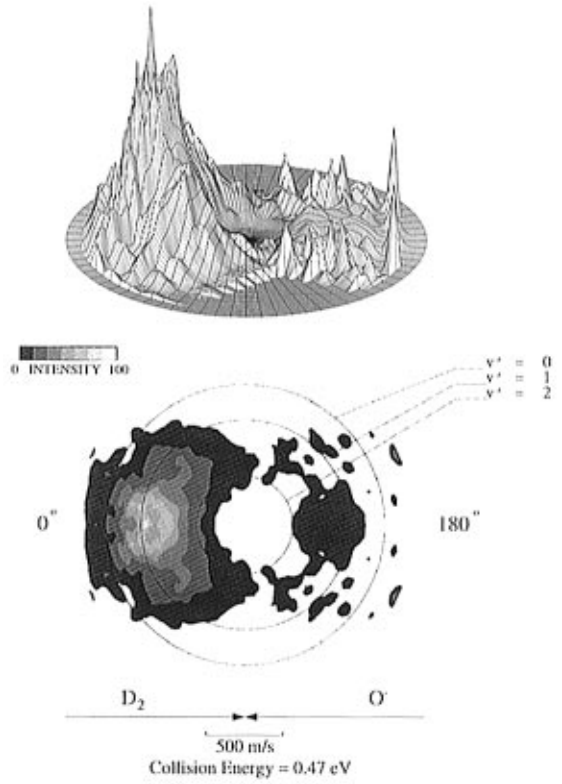

Figure 2. Axonometric plot and gray scale projection of center of mass flux in center of mass velocity space at a collision energy of 0.47 eV. Circles of constant radius corresponding to the loci of points followed by OD^- products formed in the given vibrational state with no rotational excitation are superimposed on the color projection.

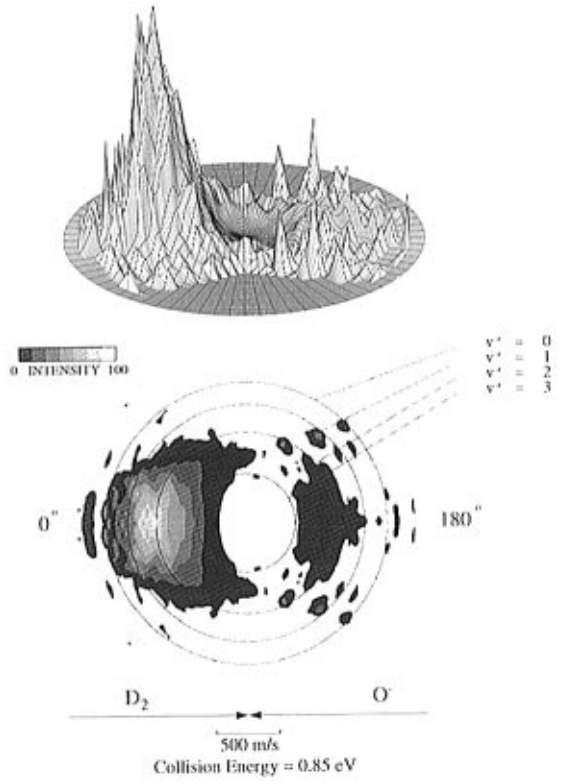

Figure 3. Same as Figure 2, at a collision energy of 0.85 eV.

typical experimental data at selected laboratory scattering angles at a collision energy of 1.20 eV for the OD^- product fluxes, compared with the results of a kinematic simulation of the center of mass distributions that have been transformed back to the laboratory system with appropriate averaging over the experimental conditions. The structure in the experimental data corresponds to OD^- produced with specific amounts of vibrational energy. The data in Figure 1 show clear structure that corresponds to the inner and outer branches of the circles describing OD^- produced with zero to four quanta of vibrational excitation.

As described in our paper on the low energy dynamics of this system, we transformed the laboratory flux distributions to the center of mass coordinate system with a pointwise iterative deconvolution procedure[12] that recovers the energy-independent differential cross section $I_{cm}(u,\theta)$ (center of mass intensity distribution) from the lab data by inverting the transformation relation 2:

$$I_{lab}(V,\Theta) = \sum_{i=1}^{N} f_i \frac{V^2}{u_i^2} I_{cm}(u_i,\theta_i) \qquad (2)$$

The summation extends over a grid of N Newton diagrams that represents the dispersion in beam velocities and intersection angles; the ith diagram is weighted by the value f_i. Details of this procedure are given in earlier publications from our laboratory,[13,14] and the results of the procedure are presented here. The $I_{cm}(u, \theta)$ generated this way is intrinsically nonseparable in the variables u and θ.

In Figures 2−4, we plot the center of mass distributions for the OD^- products. The data are plotted as a function of the polar coordinates u and θ; the vertical coordinate corresponds to the flux intensity at a particular set of coordinates. The data plotted in these figures are those resulting from direct pointwise deconvolution of the experimental data and embody the noise of the original data amplified by the deconvolution procedure.

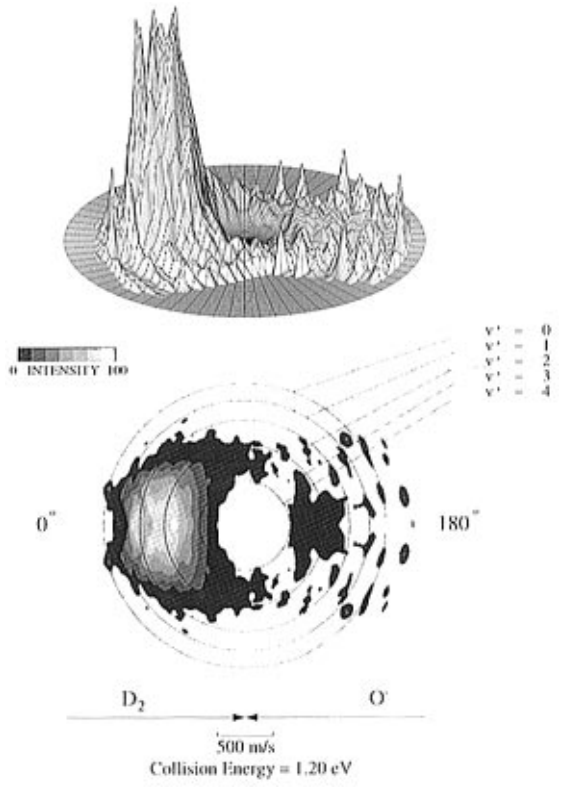

Figure 4. Same as Figure 2, at a collision energy of 1.20 eV.

We can assess qualitative features of the dynamics immediately from this representation of the data. The distributions are highly asymmetric with respect to the bisector of the relative velocity vector, indicating that the OD^- products are formed in

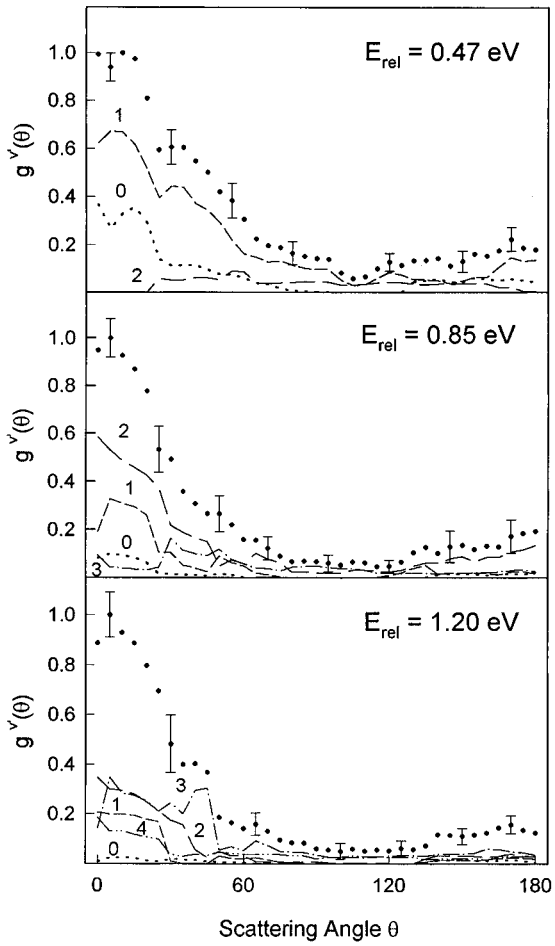

Figure 5. Angular distributions $g^{v'}(\theta)$ for each vibrational state, 0.47, 0.85, and 1.20 eV experiments, obtained from kinematic analysis. Vibrational states are labeled on the Figure: $v = 0$ (line 0) $v' = 1$: (line 1), $v' = 2$ (line 2), $v' = 3$ (line 3), $v' = 4$ (line 4). The total angular distribution is indicated by filled circles with error bars.

direct encounters that produce forward scattering. The maxima in the intensity distributions correspond to vibrationally excited OD^- products. The backward scattered product fluxes show significant structure and fluctuations in intensity, the significance of which we will address later.

Reconstructing the laboratory flux distributions by fitting the deconvoluted center of mass fluxes to a series of Gaussian functions indexed to the individual product vibrational states[13] allowed us to extract product vibrational states along with their angular dependences from the center of mass distributions. This procedure treated the center of mass flux distributions as separable product functions in recoil speed and scattering angle in small wedges of center of mass angular space,[14] typically 5°−10° in width. We recovered the coupling of recoil speed with scattering angle in the data accurately with a set of functions that varied with scattering angle. Representing the contribution of a given vibrational state in the center of mass system with an analytic function allowed us to account for the contribution of that vibration to the flux in laboratory space. The kinematic simulations that are compared with experimental data in Figure 1 are calculated with this fitting procedure. In addition, by integrating the function assigned to a particular vibration at a fixed center of mass scattering angle over the full range of center of mass speeds accessible to products in that vibrational state, the product state-resolved angular distributions $g^{v'}(\theta)$ can be constructed. The product state-resolved angular distributions extracted from the center of mass data for the accessible vibrational states are plotted in Figure 5.

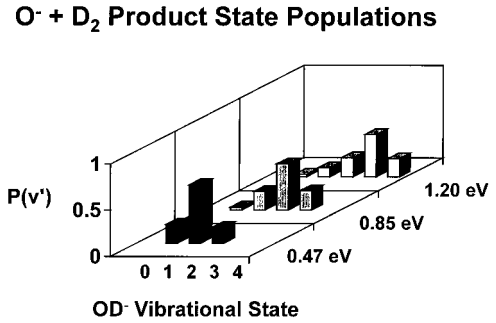

Figure 6. OD^- vibrational state distributions at each collision energy, calculated from equation (3) in text.

The probability of populating a given vibrational state is calculated by integrating the differential cross section, determined either from deconvolution of the laboratory data or by fitting the deconvoluted data to a set of Gaussian functions representing the contributions from individual vibrational states, over the full range of center of mass scattering angles, and over the range of center of mass speeds accessible to that vibrational state:

$$P(v') = \int_{u_{min}}^{u_{max}} \int_0^{2\pi} I^{v'}(u,\theta) \sin\theta \, d\theta \, du \qquad (3)$$

The results of this calculation are shown in Figure 6. At a collision energy of 0.47 eV, three product vibrational states are accessible; the number of accessible vibrational states increases to four at 0.85 eV and five at 1.20 eV. The most probable vibrational state consistently corresponds to one fewer quanta of excitation than the maximum allowed by energy conservation. The data show a consistent, monotonic increase in product vibrational excitation with increasing collision energy. As we will discuss later, the widths of the product vibrational distributions are quite likely determined by the zero point motion of the D_2 reagent.[15]

The fraction of the total available energy appearing in product vibrational energy, is defined as

$$f'_V = \frac{\sum_{v'=0}^{v'_{max}} P(v')E(v')}{E_{total}} \qquad (4)$$

where $P(v')$ represents the probability of observing a vibrational state of energy $E(v')$ and E_{total} is the total energy accessible to the system, which increases monotonically from 0.42 to 0.60 over the collision energy range reported here. This behavior contrasts markedly from that at the three lowest energies, where f_V' remained constant at approximately 30%, and provides a clear signal of a change in dynamical signature as the collision energy increases.

Angular momentum is a dynamical variable that couples mass, approach speed, and the range of the interaction potential into a single quantity with great diagnostic value. Kinetic energy distributions for individual OD^- product vibrational states are equivalent to rotational distributions for a specific vibrational state. Although the consumption of reagent rotational excitation and product angular momentum disposal is a topic sufficiently rich in dynamical detail for the present system that we have chosen to publish those details in a separate paper,[16] we summarize here a few salient characteristics of the rotational distributions. At each collision energy, the range of rotational states populated for a given product vibrational state is effectively 10−15 $\hbar$ for each vibrational state except the highest

populated one, for which the range is about 5 $\hbar$ smaller, or 5−10 $\hbar$. Rotational state populations are effectively independent of product vibrational state and collision energy. This saturation of the product rotation is consistent with the results of the *ab initio* calculations by Werner, Mänz, and Rosmus that show the low energy repulsion in the so-called "corner" of the surface softening as approach geometries become increasingly non-collinear.

IV. Discussion

The vibrational state distributions shown in Figure 5 provide a convenient starting point for discussing the dynamics of the $O^- + D_2$ system in the high energy regime. The attractive long range force in the entrance channel for this system results in an example of the "early downhill" potential energy surface, suggesting that much of the energy of the reaction is liberated while the reagents approach. Forward-scattered, vibrationally excited products are formed through large impact parameter collisions in this situation. The $O^- + D_2$ system provides an example of the Heavy + Light−Light (H + LL) mass combination[17,18] for which numerous trajectory studies on neutral−neutral systems show that a significant fraction of reactive trajectories liberate the energy of reaction while both the breaking bond in the reagent and the incipient bond of the products are extended. This so-called mixed-energy release motif also leads to the formation of vibrationally excited products. Within this picture, the widths of the product vibrational energy distributions arise from the zero-point motion of the Light−Light (LL) reagent. Corner-cutting trajectories characteristic of mixed energy release arise because the skew angle of the potential energy surface for this mass combination is approximately 48°.[19] At moderate collision energies, this acute skew angle dictates that many product trajectories enter the exit valley transverse to the reaction coordinate and form vibrationally excited products.

Although the energy partitioning predicted at a single collision energy is consistent with the occurrence of hydrogen atom transfer in corner-cutting geometries, the mixed energy release motif of atom transfer also predicts that, at higher collision energies, the moderate skew angle of the potential energy surface directs trajectories with additional reagent translation into the corner of the surface.[20] Energy is then released as the products separate, leading to translationally excited products. In the case where the collision geometries in the corner are bent, some of the reagent translation appears in product rotational excitation. Thus, classical trajectory studies show that the extent of product vibrational excitation will decrease with increasing translational energy for this particular mass combination. In fact, we observe precisely the opposite behavior: the fraction of the total energy appearing in product vibration increases monotonically from 0.42 to 0.60 over this collision energy range.

This partitioning of incremental reagent translation into product vibrational excitation is similar in nature, but almost certainly different in origin, to that observed in the low energy regime for the Heavy + Light−Heavy system $O^- + HF$.[21,22] In that system, with its significantly smaller skew angle of 19°, the deep potential energy well associated with the charge−dipole O^-·HF complex, with an HF bond distance close to its equilibrium value and an elongated O−H distance, causes most low-energy trajectories to avoid the corner of the surface. In the low-energy regime, the reagent translation, in conjunction with the acceleration of the reagents by the long range attraction, results in increased corner cutting with increased collision energy, as long as trajectories sample regions of the surface dominated by the attractive well. Only at higher translational energies[14,23] does the system reach the corner, which guides trajectories into the exit channel with enhanced translation. At that point, the system begins to explore a qualitatively new region of the potential surface, and the experimental data show that the fraction of total energy appearing in product vibration begins to fall significantly.[24]

On the one hand, the $O^- + HF$ results at low energy do compare well with the $O^- + D_2$ results reported here, in that incremental translation appears in product vibration. The long range force in the $O^- + D_2$ system, albeit much weaker than in $O^- + HF$, may cause atom transfer to occur for extended reagent and product bond distances. On the other hand, the collision energy range in the $O^- + D_2$ system extends to significantly higher energies than in $O^- + HF$, and the well depths of the electrostatically bound intermediates are much smaller in the present system. Certainly the system does explore the low-energy repulsion and the corner of the surface in the $O^- + D_2$ case. The increase in product vibration is clearly at odds with the conventional classical picture in which the low-energy repulsion directs reagent translation into product translation. The fraction of available energy in vibrational excitation appears to level off at the highest collision energy of 1.2 eV; that behavior may precede the expected decrease in product vibrational excitation, but we have no experimental observations to support that claim. Even if higher energy experiments show such behavior, we are surprised that the high level of product vibrational excitation persists to such a high collision energy. Above a total energy of 1.8 eV, the electron affinity of OH,[25] the electron may autodetach in most highly vibrationally excited states,[26] but the total energies in our experiments do not exceed this threshold.

Vibrationally resolved angular distributions for the experiments at 0.47, 0.85, and 1.20 eV are shown in Figure 5. Generally, we observe that the $v' = 0$ state shows both forward and backward peaks, with the forward component dominating at all collision energies. The highest vibrational state accessible to the products increases from 2 to 3 to 4 over the three collision energies, and this most highly excited state typically has a fairly flat angular distribution with some energy dependent structure in the sideways direction. At 0.85 eV, the $v' = 3$ state shows some modulation of intensity in the sideways direction. The lowest three vibrational states also show sharps spikes of intensity at approximately 150°, seen clearly in the flux plot of Figure 3. At the highest collision energy, the $v' = 3$ state shows two fairly sharp structures in the angular range between 20° and 60°. All of the structures are reproducible and physically significant, but unlike the angular distributions at the lower collision energies which could be thought of, in part, in terms of transient complex lifetimes, no ready physical interpretation is available. The intensity modulations may be manifestations of quantum interference phenomena. Testing this conjecture will require detailed quantum-scattering calculations.

V. Conclusions

The experimental data presented on the $O^- + D_2$ reaction in the moderate collision energy regime from 0.47 to 1.20 eV show the onset of direct reaction dynamics and enhanced product vibrational excitation with increasing collision energy. The fraction of the available energy appearing in product vibration increases smoothly from 0.42 to 0.60 over this collision energy range. At a fixed collision energy, the formation of vibrationally excited products is consistent with the mechanism of mixed energy release, in which the atom transfer process occurs with both the breaking bond in the reagents and the incipient bond in the products in an extended configuration. However, the

increase in product vibrational excitation with collision energy, while consistent with intermediate energy results on the $O^- +$ HF system,[22] is not consonant with the results of trajectory studies indicating that incremental translation in the Heavy + Light−Light system appears in product translation as the corner of the surface controls the dynamics. This deviation suggests that other regions of the potential surface are equally important in determining how energy is partitioned in this system. Consistent with the important role of the low-energy repulsion, however, is the observation that the most probable product rotational quantum numbers are sensibly independent of product vibrational state and collision energy. The decrease in slope of the low-energy repulsion in the surface corner in more bent geometries is consistent with this observation.

The present data, which probe the low-energy repulsive regions of the potential surface, in conjunction with our study over a lower collision energy range in which the bending potential in the vicinity of the collinear OD^-•D configuration controls the branching ratio for particle transfer relative to electron detachment, provide an extraordinarily detailed picture of the dynamics of this interesting system. We hope these data will inspire structural and dynamical calculations on this interesting system.

Acknowledgment. We acknowledge support of this work by the U.S. Department of Energy. M.A.C. expresses thanks to the University of Rochester for Fellowship support from the Sherman Clarke and Weissberger Funds. We thank Marty Zanni, Susan Troutman Lee, and David Sperry for their assistance in the performing and analysis of these experiments. J.M.F. thanks Professor Richard N. Zare for helpful comments and also Professors Franco Vecchiocattivi, Enzo Aquilanti, Piero Casavecchia, and Antonio Laganà of the University of Perugia for continuing conversations. He also acknowledges a NATO Collaborative Research Grant.

References and Notes

(1) Carpenter, M. A.; Farrar, J. M. *J. Phys. Chem.* **1997**, *101*, in press. This paper provides much of the relevant literature background for the present study.

(2) Carpenter, M. A.; Zanni, M. T.; Farrar, J. M. *J. Phys. Chem.* **1995**, *99*, 1380.

(3) Levine, R. D.; Bernstein, R. B. *Acc. Chem. Res.* **1980**, *12*, 393. Levine, R. D.; Bernstein, R. B. *J. Chem. Phys.* **1972**, *57*, 434. Levine, R. D., Kinsey, J. L. In *Atom-Molecule Collision Theory: A Guide for the Experimentalist;* Bernstein, R. B., Ed.; Plenum: New York, 1979; p 693.

(4) Werner, H. -J.; Mänz, U.; Rosmus, P. *J. Chem. Phys.* **1987**, *87*, 2913.

(5) Mauer, J. L.; Schulz, G. J. *Phys. Rev. A* **1972**, *7*, 593.

(6) Allan, M. *Chimia* **1982**, *36*, 457.

(7) Herbst, E.; Payne, L. G.; Champion, R. L.; Doverspike, L. D. *Chem. Phys.* **1979**, *42*, 413.

(8) Johnson, S. G.; Kremer, L. N.; Metral, C. J.; Cross, R. J., Jr. *J. Chem. Phys.* **1978**, *68* 1444.

(9) Varley, D. F.; Levandier, D. J.; Farrar, J. M. *J. Chem. Phys.* **1992**, *96*, 8806.

(10) Gallagher, R. J.; Fenn, J. B. *J. Chem. Phys.* **1974**, *60*, 3487, 3492.

(11) Varley, D. F.; Levandier, D. J.; Farrar, J. M. *J. Chem. Phys.* **1992**, *96*, 8806.

(12) Siska, P. E. *J. Chem. Phys.* **1973**, *59*, 6052.

(13) The details of the procedure are given in Carpenter, M. A. Ph.D. dissertation, University of Rochester, 1996 (published by University Microfilms).

(14) Carpenter, M. A.; Zanni, M. T.; Levandier, D. J.; Varley, D. F.; Farrar, J. M. *Can. J. Chem.* **1994**, *72*, 828.

(15) Polanyi, J. C.; Schreiber, J. L. *J. Chem. Soc., Faraday Discuss.* **1977**, *62*, 267.

(16) Carpenter, M. A.; Farrar, J. M. unpublished data.

(17) Kuntz, P. J.; Nemeth, E. M.; Polanyi, J. C.; Rosner, S. D.; Young, C. E. *J. Chem. Phys.* **1966**, *44*, 1168.

(18) Polanyi, J. C. *Acc. Chem. Res.* **1972**, *5*, 161.

(19) Eyring, H.; Polanyi, J. C. *Z. Phys. Chem.* **1931**, *B12*, 279. Mahan, B. H. *J. Chem. Educ.* **1974**, *51*, 308, 377.

(20) Ding, A. M. G.; Kirsch, L. J.; Perry, D. S.; Polanyi, J. C.; Schreiber, J. L. *J. Chem. Soc., Faraday Discuss.* **1973**, *55*, 252.

(21) Hamilton, C. E.; Duncan, M. A.; Zwier, T. S.; Weisshaar, J. C.; Ellison, G. B.; Bierbaum, V. M.; Leone, S. R. *Chem. Phys. Lett.* **1983**, *94*, 4.

(22) Knutsen, K.; Bierbaum, V. M.; Leone, S. R. *J. Chem. Phys.* **1992**, *96*, 298.

(23) Levandier, D. J.; Varley, D. F.; Carpenter, M. A.; Farrar, J. M. *J. Chem. Phys.* **1993**, *99*, 148.

(24) Chapman, S.; Ali, D. P.; Hynes, J. T. *Chem. Phys.* **1989**, *136*, 2971.

(25) Hotop, H.; Patterson, T. A.; Lineberger, W. C. *J. Chem. Phys.* **1974**, *60*, 1809.

(26) Simons, J. P. *J. Am. Chem. Soc.* **1981**, *103*, 3971. Acharya, P. K.; Kendall, R. A.; Simons, J. *J. Am. Chem. Soc.* **1984**, *106*, 3402.